Optics Letters

Polarization properties of the Airy beam

SEAN NOMOTO, A. AADHI, SHASHI PRABHAKAR, R. P. SINGH, REETA VYAS, AND SURENDRA SINGH

¹Department of Physics, University of Arkansas, Fayetteville, Arkansas 72701, USA

²Atomic, Molecular and Optical Physics Division, Physical Research Laboratory, Ahmedabad 380009, India

*Corresponding author: rvyas@uark.edu

Received 29 June 2015; revised 27 August 2015; accepted 2 September 2015; posted 3 September 2015 (Doc. ID 243478); published 29 September 2015

Polarization of paraxial Airy beam solutions of Maxwell's equations and its evolution with propagation have been studied. We experimentally demonstrate the existence of the cross-polarization component of the Airy beam, typical of nonplanar phase fronts, and study its evolution with propagation. © 2015 Optical Society of America

OCIS codes: (260.0260) Physical optics; (260.5430) Polarization; (140.3300) Laser beam shaping.

http://dx.doi.org/10.1364/OL.40.004516

Following the observation of the Airy light beam by Siviloglou et al. [1], inspired by the prediction of its quantum mechanical analog by Berry and Balazs [2], its unusual and interesting properties and their applications have been the subject of numerous investigations [3–9]. These include self-healing, autofocusing, and self-acceleration of the Airy beam and its application in particle accelerators and beam arrays. On the other hand, its polarization properties have not yet received much attention. While many of the properties referred to above can be understood in the context of the Airy beam as a solution to the paraxial scalar wave equation, its inhomogeneous polarization due to nonplanar phase fronts requires its vector character to be taken into account. A consequence of this is coupling of polarization and spatial degrees of freedom of light via Maxwell's equations, $\vec{\nabla} \cdot \vec{E} = 0$ and $\vec{\nabla} \cdot \vec{B} = 0$, leading to a nonzero crosspolarization component for a predominantly linearly polarized beam. The presence of a cross-polarization (CP) component for Hermite-Gauss (HG) and Laguerre-Gauss (LG) beams has been observed experimentally [10–14]. Polarization components for cylindrically polarized Bessel-Gauss and Laguerre-Gauss beams have been investigated by Lewis and Vyas [15]. In this article, we investigate the transverse spatial profiles of the dominant polarization (DP) and CP components, and their evolution with propagation for a linearly polarized Airy beam experimentally and compare with the theoretical predictions.

The scalar wave equation for a wave traveling predominantly in the z direction, derived from the free-space Maxwell's equations in the paraxial approximation, may be written as [16]

$$\left[\nabla_{\perp}^{2} + 2ik\frac{\partial}{\partial z}\right]\psi(\vec{r}) = 0.$$
 (1)

Here, $k = 2\pi n/\lambda$ is the wavenumber, n is the refractive index of the medium of propagation, and λ is the wavelength of light. Introducing dimensionless scaled variables $\tilde{x} = x/x_0$, $\tilde{y} = y/x_0$, and $\tilde{z} = z/kx_0^2$, with the scale length x_0 still to be specified, the paraxial wave equation can be written as

$$\left[\frac{\partial^2}{\partial \tilde{x}^2} + \frac{\partial^2}{\partial \tilde{y}^2} + 2i\frac{\partial}{\partial \tilde{z}}\right]\psi(\vec{r}) = 0.$$
 (2)

For Airy beam solutions of this equation, we look for separable solutions of the form $\psi(\vec{r}) = u_r(\tilde{x}, \tilde{z})u_v(\tilde{y}, \tilde{z})$. Substituting this in Eq. (2) and separating the variables, we find that $u_r(\tilde{x}, \tilde{z})$ and $u_{\nu}(\tilde{y}, \tilde{z})$ must satisfy the following equations:

$$\left[\frac{\partial^2 u_x}{\partial \tilde{x}^2} + 2i \frac{\partial u_x}{\partial \tilde{z}} \right] = 0,$$

$$\left[\frac{\partial^2 u_y}{\partial \tilde{y}^2} + 2i \frac{\partial u_y}{\partial \tilde{z}} \right] = 0,$$
(3)

where the constant of separation has been chosen to be zero, and for simplicity we have suppressed arguments of u_x and u_y . One possible solution of these differential equations can be expressed in terms of the Airy functions with the initial conditions (in the z = 0 plane) [1,2]

$$u_x(\tilde{x}, 0) = \operatorname{Ai}[\tilde{x}]e^{a\tilde{x}},$$

$$u_y(\tilde{y}, 0) = \operatorname{Ai}[\tilde{y}]e^{a\tilde{y}},$$
(4)

where $Ai(\tilde{x})$ denotes the Airy function [17] with argument \tilde{x} . The parameter a is the effective aperture of the beam, which ranges from 0 to 1 and truncates the Airy beam for negative values \tilde{x} , $\tilde{y} < 0$. For a = 0, we recover an ideal (infinite) Airy beam, whereas for $a \approx 1$ it approaches essentially a single-lobe beam. An infinite Airy beam, like an infinite plane beam, is unrealistic, as it would carry infinite power. The solution of the differential equation at finite z is obtained by using the Huygen-Fresnel integral to be

$$u(\tilde{x}, \tilde{z}) = \sqrt{\frac{i}{2\pi\tilde{z}}} \int_{-\infty}^{+\infty} dx' u_x(x', 0) \exp\left[\frac{i}{2\tilde{z}} (x' - \tilde{x})^2\right],$$

$$= \operatorname{Ai}\left[\tilde{x} + ia\tilde{z} - \left(\frac{\tilde{z}}{2}\right)^2\right]$$

$$\times \exp\left[a\left(\tilde{x} - \frac{\tilde{z}^2}{2}\right) + i\left(\frac{\tilde{x}\,\tilde{z}}{2} + \frac{a^2\tilde{z}}{2} - \frac{\tilde{z}^3}{12}\right)\right].$$
(5)

Replacing \tilde{x} by \tilde{y} in Eq. (5), we obtain the expression for $u(\tilde{y}, \tilde{z})$. Thus, the scalar Airy beam can be expressed as [18]

$$\psi(\vec{r}) = \operatorname{Ai}\left[\tilde{x} + ia\tilde{z} - \left(\frac{\tilde{z}}{2}\right)^{2}\right] \operatorname{Ai}\left[\tilde{y} + ia\tilde{z} - \left(\frac{\tilde{z}}{2}\right)^{2}\right]$$

$$\times \exp\left[a\left(\tilde{x} - \frac{\tilde{z}^{2}}{2}\right) + i\left(\frac{\tilde{x}\tilde{z}}{2} + \frac{a^{2}\tilde{z}}{2} - \frac{\tilde{z}^{3}}{12}\right)\right]$$

$$\times \exp\left[a\left(\tilde{y} - \frac{\tilde{z}^{2}}{2}\right) + i\left(\frac{\tilde{y}\tilde{z}}{2} + \frac{a^{2}\tilde{z}}{2} - \frac{\tilde{z}^{3}}{12}\right)\right].$$
 (6)

To construct paraxial vector solutions of Maxwell equations in terms of these solutions, we follow Erikson and Singh [10] expanding the field components in powers of $(1/kx_0)$. Assuming that the Airy beam is predominantly polarized in the x direction, in the paraxial approximation, the cross (y) and longitudinal (z) polarization components can be written as

$$E_x \approx \psi(\tilde{x}, \tilde{y}, \tilde{z}),$$
 (7)

$$E_{y} \approx \frac{1}{2(kx_{0})^{2}} \frac{\partial^{2}}{\partial \tilde{x} \partial \tilde{y}} \psi(\tilde{x}, \tilde{y}, \tilde{z}),$$
 (8)

$$E_z \approx \frac{i}{kx_0} \frac{\partial}{\partial \tilde{x}} \psi(\tilde{x}, \tilde{y}, \tilde{z}),$$
 (9)

where ψ is the scalar field solution given in Eq. (6). Intensity distributions of the three polarization components are proportional to the absolute square of the field components given by Eqs. (7)–(9). For the dominant and cross-polarization (DP and CP, respectively) components, these are given by

$$I_{x} \propto \left| \operatorname{Ai} \left[\tilde{x} + ia\tilde{z} - \left(\frac{\tilde{z}}{2} \right)^{2} \right] \operatorname{Ai} \left[\tilde{y} + ia\tilde{z} - \left(\frac{\tilde{z}}{2} \right)^{2} \right] \right|^{2}$$

$$\times \exp[a(2\tilde{x} + 2\tilde{y} - 2\tilde{z}^{2})], \tag{10}$$

$$I_{y} \propto \frac{1}{4(kx_{0})^{4}} \exp[a(2\tilde{x} + 2\tilde{y} - 2\tilde{z}^{2})]$$

$$\times \left| \left(a + i\frac{\tilde{z}}{2} + \frac{\partial}{\partial \tilde{x}} \right) \operatorname{Ai} \left[\tilde{x} + ia\tilde{z} - \left(\frac{\tilde{z}}{2} \right)^{2} \right] \right|^{2}$$

$$\times \left| \left(a + i\frac{\tilde{z}}{2} + \frac{\partial}{\partial \tilde{y}} \right) \operatorname{Ai} \left[\tilde{y} + ia\tilde{z} - \left(\frac{\tilde{z}}{2} \right)^{2} \right] \right|^{2}.$$
(11)

Figure 1 shows intensity profiles for the DP and CP components at beam waist $\tilde{z} = 0$ for aperture parameter values a = 0.1, 0.5, and 0.9. The pattern for the CP component appears shifted relative to the DP component, and the main corner lobe is significantly weak. Each lobe in the DP component appears to split into four asymmetric lobes of unequal intensities in the CP. As a increases from 0.1 to 0.9, this splitting behavior continues, but beam extent and the number of lobes are reduced. In fact, as a approaches unity, the crosspolarization intensity pattern resembles that of an asymmetric Gaussian beam [10-14].

In addition to the evolution of the DP and CP intensity profiles with propagation, another unusual characteristic of the Airy beam is its self-acceleration property, which is reflected in its parabolic trajectory [1]. In one dimension, the deflection, x_d , of the Airy beam follows a parabolic path [3]:

$$x_d = \theta z + \frac{z^2}{4 \ k^2 x_0^3},\tag{12}$$

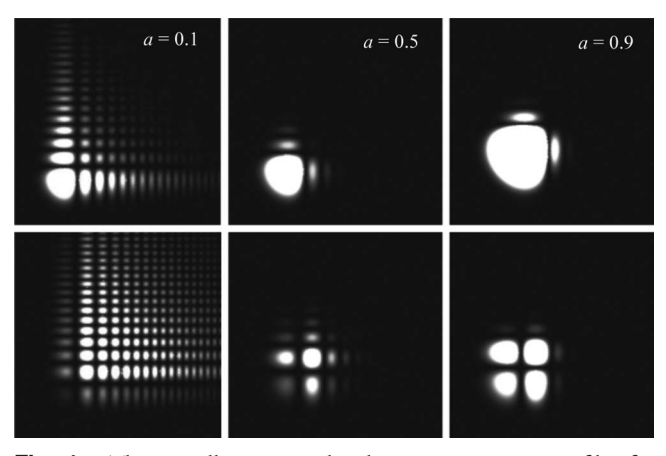


Fig. 1. Theoretically computed polarization intensity profiles for the DP (top row) and CP (bottom row) components (left to right) for a = 0.1, 0.5, 0.9 at $\tilde{z} = 0$.

where θ is the launch angle with respect to the +z axis, k is the wavenumber, and x_0 is the scaling factor introduced in Eq. (2). In the next section, we describe experiments to observe these features related to polarization intensity profiles and beam trajectory.

Figure 2 shows an outline of the experimental setup. A linearly polarized 50 mW of 633 nm He–Ne laser beam of nominally 2 mm diameter was incident on a BNS 512 phase-only spatial light modulator (SLM). The LCD array of the SLM has dimensions of 7.68 mm \times 7.68 mm with pixel pitch of 15 μ m \times 15 μ m. A half-wave plate was used to adjust the incident beam polarization to match the polarization required by the SLM for optimum phase modulation. A blazed cubic phase grating, given by [19]

$$\phi(x,y) = \frac{2\pi x}{\Lambda} + \frac{x^3 + y^3}{R^3},$$
(13)

corresponding to the Airy beam, was written on the SLM to modulate the incident Gaussian beam phase. Here, Λ is the grating period, R is a parameter controlling the curvature of the cubic phase modulation, and x and y are the coordinates of a point on the LCD array. Increasing R decreases the cubic modulation and yields Airy beams with a close to 1, whereas decreasing R increases the modulation yielding Airy beams with a close to 0. The grating period was kept fixed to ensure that the first-order diffraction appeared in the same direction.

The first-order diffracted beam from the SLM was passed through a lens placed one focal length (f = 50 cm) away from the SLM. The Airy beam was produced in the back focal plane of the lens at a distance of 2f from the SLM. The back focal plane of the lens defined the plane $z = 0 = \tilde{z}$. A CCD

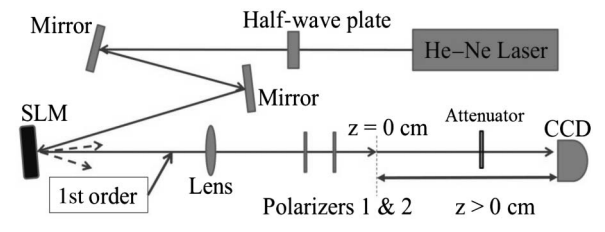


Fig. 2. Outline of the experimental setup.

camera (Spiricon 480M) recorded the intensity profiles of the polarization components at different distances z for a = 0.11, 0.22 and 0.97. The intensity profiles of the dominant polarization component were recorded with the transmission axes of both linear polarizers (Meadowlark Optics) aligned with the dominant polarization direction. To measure the crosspolarization intensity profile, the second polarizer was oriented such that its transmission axis was crossed relative to the first. The extinction ratio of the polarizers in the experiment was 10^5 . An attenuator (a neutral density filter) in front of the CCD was used to adjust the light level reaching the detector.

The trajectory of the dominant polarization component of the Airy beam was measured relative to the trajectory of a first-order Laguerre–Gauss (LG) beam produced by the same method as the Airy beam but with a forked grating phase mask with $\ell=1$ [20,21]. As the LG beam propagates along a straight-line trajectory, it was used as the reference for measuring the Airy beam trajectory. The first-order LG beam was chosen over the zeroth-order Gaussian because all phase masks used were blazed, and the Airy beam and Gaussian could not be recorded at the propagation distance without translating the CCD in the transverse direction.

Experimentally recorded intensity profiles of the dominant and cross-polarization components were compared with those obtained from Eqs. (10) and (11). This required a determination of the aperture and scaling parameters a and x_0 . These were determined by fitting line profiles of the DP component intensity to the curve obtained from Eq. (10) for $\tilde{z}=0$. To further refine x_0 , the transverse displacement of the central peak of the Airy beam was measured relative to the center of a first-order LG beam. The first-order Airy beam appeared in a slightly different direction α relative to the first-order LG beam. The deflection of the Airy beam was calculated by

$$r_d = r_{\rm rel} + \sqrt{2}\alpha z_{\rm slm}, \tag{14}$$

where $r_{\rm rel}$ is the distance between the dominant corner peak of the Airy beam and center of the LG beam, $z_{\rm slm}$ is the distance from the SLM to the plane of observation, and α is the angle between the LG and Airy beams in the first order of diffraction. The factor of $\sqrt{2}$ accounts for the fact that the calculated trajectory is two-dimensional in the plane transverse to the propagation direction. Figure 3 shows the measured values of r_d along with the parabolic curve in Eq. (12) ($\theta=0$) for the Airy beam for three different values of aperture parameter a. The two appear to be in good agreement in all cases.

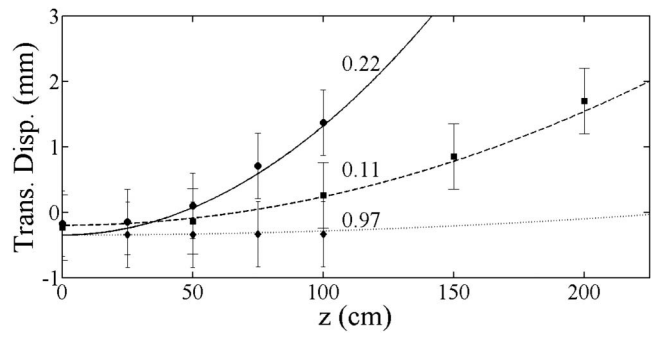


Fig. 3. Transverse displacement of the Airy beam as a function of propagation distance for three values of a as labeled. Full curves are derived from Eq. (12).

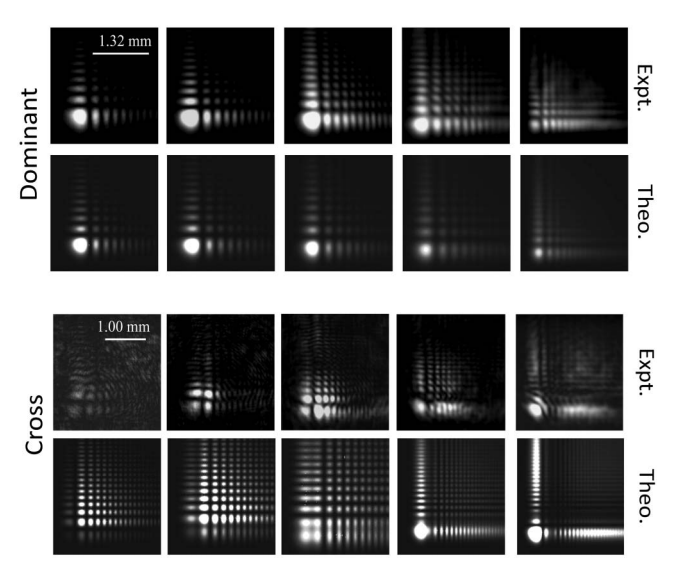


Fig. 4. Evolution of dominant and cross-polarization intensity profiles with propagation distance (left to right) z=0,50,100,150,200 cm for a=0.11. The top two rows show the experimentally measured and theoretically predicted profiles for the DP component; the bottom two rows show the corresponding CP component profiles. Scaling parameter for these profiles was $x_0=220~\mu m$.

Experimentally measured intensity profiles for the DP and CP components of the Airy beam are shown alongside the theoretically computed intensity profiles [from Eqs. (10) and (11)] in Figs. 4–6 for a = 0.11, 0.22, and 0.97 for different propagation distances.

The experiments demonstrate the inhomogeneity of polarization of the Airy beam and, in particular, the existence of its cross-polarization component as well as its evolution with propagation distance. For small a (0.11), the intensity profile of the DP component is closer to that of an ideal Airy beam

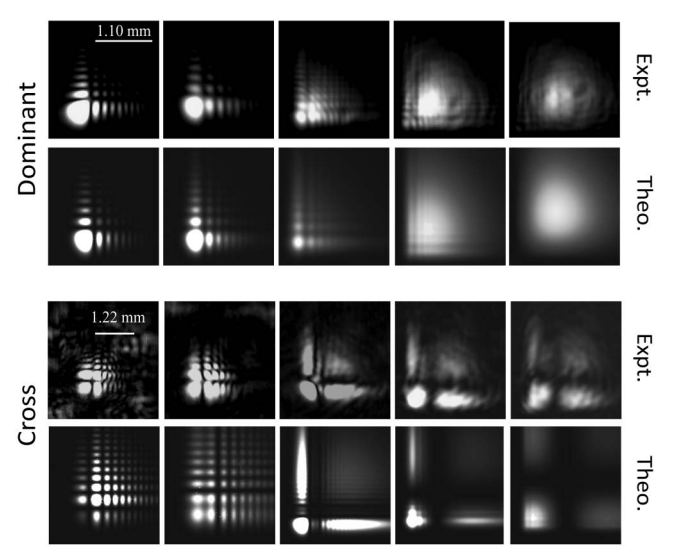


Fig. 5. Intensity profiles of the DP and CP components for (from left to right) z = 0, 25, 50, 75, 100 cm for a = 0.22. Scaling parameter for these figures was $x_0 = 130$ μ m.

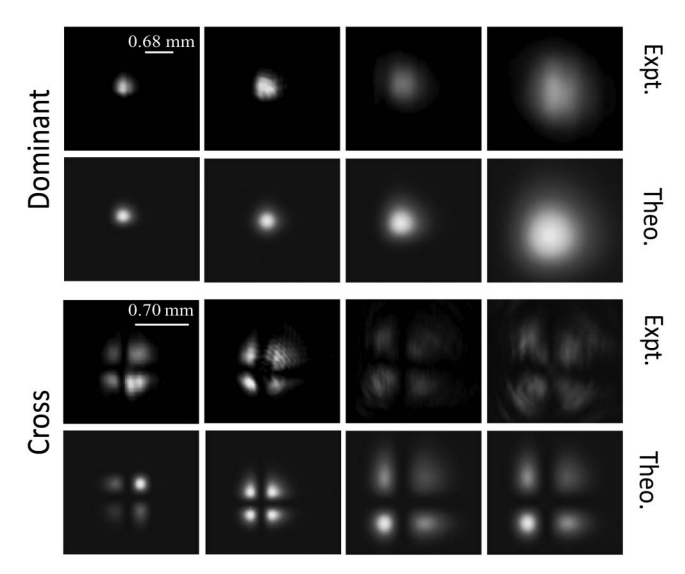


Fig. 6. Intensity profiles of the DP and CP components for (from left to right) z = 0, 25, 50, 75 cm for a = 0.97. Scaling parameter was determined to be $x_0 = 110 \ \mu \text{m}$.

with a large number of peaks and propagates farther without significant diffraction. The CP intensity shows a similar behavior with the added feature that each DP peak splits into four asymmetric lobes. With increasing propagation distance, the CP intensity approaches an intensity pattern similar to that of the CP component of a Gaussian beam. With increasing aperture parameter a (0.22), the DP intensity profile has a significantly reduced number of peaks and diffracts faster. The CP intensity profile shows similar behavior with splitting peaks. For large $a \approx 1$, the intensity profiles for both DP and CP components appear similar to those for an asymmetric Gaussian beam. For all values of a used in the experiment, the intensity profiles for both DP and CP components—their spatial structure and evolution with propagation—are found to be in agreement with the theoretical predictions. It is worth mentioning that in self-healing or self-acceleration of an Airy beam, the behavior of cross-polarization component is governed by the dominant component via Eq. (8).

Finally, we mention that Airy beams with embedded vortices (Airy vortex) are an interesting recent development [22]. Based on the results of our Letter, we expect that the behavior of cross polarization for an Airy vortex beam with dominant

linear polarization will be similar to that observed in [12–14] for Laguerre–Gauss vortex beams. For other spatially varying dominant polarizations (radial, azimuthal, etc.), the results will be more complex [15].

Funding. Physical Research Laboratory, Ahmedabad, India; National Science Foundation (NSF) (OISE 0728235).

REFERENCES

- S. A. Siviloglou, J. Broky, A. Dogariu, and D. N. Christodoulides, Phys. Rev. Lett. 99, 213901 (2007).
- 2. M. V. Berry and N. L. Balazs, Am. J. Phys. 47, 264 (1979).
- S. A. Siviloglou, J. Broky, A. Dogariu, and D. N. Christodoulides, Opt. Lett. 33, 207 (2008).
- C. Hwang, D. Choi, K. Kim, and B. Lee, Opt. Express 18, 23504 (2010)
- M. Mazilu, J. Baumgartl, and K. Dholakia, Nat. Photonics 2, 675 (2008).
- Y. Fan, J. Wei, J. Ma, Y. Wang, and Y. Wu, Opt. Lett. 38, 1286 (2013).
- P. Zhang, J. Prakash, Z. Zhang, M. S. Mills, N. K. Efremidis, D. N. Christodoulides, and Z. Chen, Opt. Lett. 36, 2883 (2011).
- 8. N. K. Emfremidis, Opt. Lett. 36, 3006 (2011).
- T. Vettenburg, H. I. C. Dalgarno, J. Nylk, C. Coll-Llado, D. E. K. Ferrier, T. Cizmar, F. J. Gunn-Moore, and K. Dholakia, Nat. Methods 11, 541 (2014).
- 10. W. L. Erikson and S. Singh, Phys. Rev. E 49, 5778 (1994).
- J. W. Moore, R. Vyas, and S. Singh, *Proceedings of Hall Symposium*,
 J. C. Begquist, S. A. Diddams, L. Hollberg, C. Oates, J. Ye, and
 L. Kaleth, eds. (World Scientific, 2006), pp. 97–99.
- R. Vyas and S. Singh, Coherence and Quantum Optics IX,
 N. P. Bigelow, J. H. Eberly, and C. R. Stroud, eds. (AIP, 2008),
 pp. 344–345.
- 13. J. Conry, R. Vyas, and S. Singh, J. Opt. Soc. Am. A 29, 579 (2012).
- 14. J. Conry, R. Vyas, and S. Singh, J. Opt. Soc. Am. A 30, 821 (2013).
- 15. W. Lewis and R. Vyas, J. Opt. Soc. Am. A 31, 1595 (2014).
- 16. P. W. Milonni and J. H. Eberly, Lasers (Wiley, 1988), Chap. 14.
- F. W. J. Olver, D. W. Lozier, R. F. Boisvert, and C. W. Clark, eds., *NIST Handbook of Mathematical Functions* (Cambridge University, 2010), Chap. 9.
- J. E. Morris, M. Mazilu, T. Cizmar, and K. Dholakia, Opt. Express 17, 13236 (2009).
- 19. G. Porat, I. Dolev, O. Barlev, and A. Arie, Opt. Lett. 36, 4119 (2011).
- J. Arlt, K. Dholakia, L. Allen, and J. Padgett, J. Modern Opt. 45, 1231 (1998).
- H. He, N. R. Heckenberg, and H. Rubinsztein-Dunlop, J. Modern Opt. 42, 217 (1995).
- 22. J. Zhou, Y. Liu, Y. Ke, H. Luo, and S. Wen, Opt. Lett. 40, 3193 (2015).